Universe
Scientific Publishing

In-Situ Measurements on Shock Wave Attenuation Rules Generated by Discontinuity Structures in Coal and Rock Medium

Hongwei Lian [1], Peng Li [2], Zhenwu Li [3], Jianhua Wang [4], Caiping Lu [1]

1. School of Mines, China University of Mining and Technology, Xuzhou 221116, Jiangsu, China.
2. Bayangaole Coal Mine, Ordos, Nei Monggol 010013, China.
3. Jining Coal Mine Group, Jining, Shandong 272073, China.
4. Xiaoyun Coal Mine, Jining, Shandong 273513, China.

Abstract: The effective weakening and controlling of mining-induced shock wave intensity is a key issue to prevent the coal and rock dynamic disasters such as rockburst and mining tremors, etc. By field measurements, the attenuation rules of shock waves generated by blast were analyzed in the coal mines with strong rockburst danger. We obtained main conclusions are as: (1) The vertical attenuation coefficient of transverse propagation is much larger than bed-parallel horizontal attenuation coefficient.(2)For the same propagation distances, there may be a significant difference of 15 times between horizontal and vertical energy attenuation coefficients; (3) along with the propagation of shock wave, the high-frequency components gradually attenuate, and the frequency spectrums move to low-frequency band.

Keywords: Shock Wave; Discontinuity Structure; Attenuation Effect; Frequency-Spectrum Evolution; In-Situ Measurements

1. Introduction

It is generally known that rockburst is triggered by the combination effect of dynamic and static stress, in which the dynamic load accompanied with shock wave is an active factor of inducing rockburst disaster and can cause the avalanche failure of coal and rock mass in the higher static stress concentration state. Therefore, how to mitigate and control the residual shock intensity after attenuation is a key issue to prevent effectively rockburst in coal mines. Blast-induced ground vibrations and their mitigation have been discussed by many researchers [1-5]. Khandelwal and Singh [6] presented the application of neural network (ANN) for the prediction of ground vibration and frequency by all possible influencing parameters of rock mass, explosive characteristics and blast design. Wei et al. [7] carried out the numerical simulations using the transient dynamic finite element program ANSYS-LSDYNA, based on the numerical results an empirical formula considering the effects of loading density, rock mass rating (RMR) and weight of charge was obtained to estimate the damage zone in granite by explosion. Khandelwal [8] demonstrated that support vector machine is capable of solving problems on the prediction of blast induced ground vibrations. Choi et al.

This paper is related to the propagation and attenuation laws of shock waves generated by relieve shot. By MS monitoring systems, using the methodology of field measurements, the shock signals were recorded and comparatively analyzed in 7206 working face of Sanhejian coal mine (SCM). The frequency-spectrum evolution rules of MS signals were demonstrated accompanied with propagation and attenuation of shock wave, and the relationship between the discontinuities and the attenuation coefficients was established as well in this paper.

2. Attenuation effect of goaf and roadway to blast-induced shock wave

2.1 In-situ geological condition

SCM is one of the most serious rockburst coal mines in China. This field experimental study on the attenuation of blast-induced shock wave was conducted in 7206 working face headentry, and the average elevation of which is -840 m (the average elevation of corresponding surface is +36 m).The average thickness of the mining 7# coal seam is 2.25 m, and the

dip is from 19° to 38° with the average of 29°. The immediate roof is siltstone with the average thickness of 3 m. The primary roof is medium sandstone, and the thickness is 11.89-18.06 m with the average of 12.97 m. The immediate floor is siltstone, and the average thickness is 4.3 m.

We designed a 5 m width coal pillar left between 7206 working face headentry and the adjacent 7204 working face tailentry. In 2001, 7204 working face has been mined out. Except the goaf side, the rest sides of 7206 working face are real coal materials. The explosion is the normal driving blasting. Generally, 5-6 holes were drilled ahead of 7206 working face headentry, and the total charge weight was 12-15 kg, which was detonated simultaneously. Fig.1 is the plane sketch of 7206 working face headentry in the process of driving.

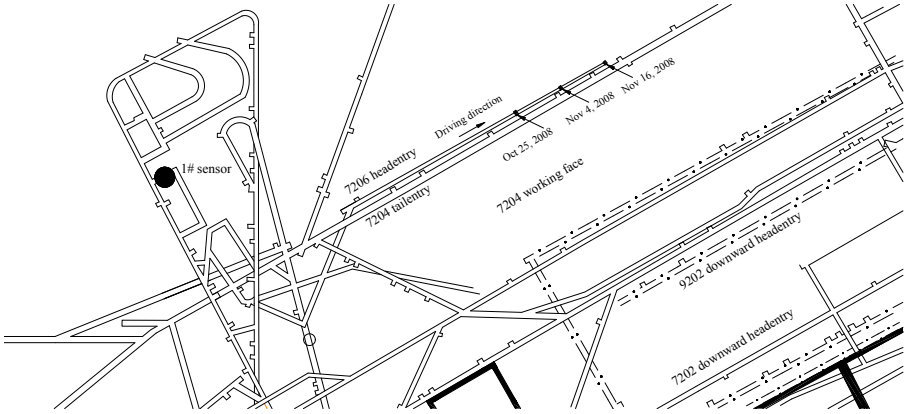

Fig.1. Roadways plane arrangement of testing area

2.2 Microseismic system and stations arrangement

KZ-1 MS monitoring system was applied in coal mine. Total six three-component sensors were installed around 7206 working face, which were named 1#, 3#, 4#, 8#, 10#, and 12# stations (8# station is named Meiqizhan, and 12# station is named Luxinzhuang), respectively. To achieve the purpose of improving the sensitivity of the system, all underground sensors were installed in the 5-10 m deep boreholes. This experimental study mainly analyzed MS data collected by 1#, 3#, 4# and 8# stations. Tab.1 shows the three-dimensional coordinates of the above-mentioned 4 sensors.

Tab.1 The three-dimensional coordinates of 4 sensors

Sensor number	Coordinates		
	x/m	y/*m*	z/*m*
1#	3864466.831	39478794.5	-902.2
3#	3863577.653	39478134.35	-734.5
4#	3864772.992	39479980.53	-742.157
8#	3865859.52	39479664.37	-192.15

From the explosion source to 1# and 3# sensors, the regular propagation path of shock wave will pass through the physical coal material and 7204 working face goaf (including many roadways), respectively. Similarly, from the explosion source to 4# sensor, the regular propagation path of shock wave will pass through in sequence the goafs of 9202, 7202 and 7204 working faces. Another, from the explosion source to 8# sensor, the propagation of shock wave will be, mainly and vertically, attenuated by the interface between coal seam and rock strata.

2.3 Explosion experiments and analysis

we drilled five blast holes in the headentry of 7206 working face on Oct 25, 2008, and the total charge weight was 15 Kg.

After explosion, the fall length of roof in the driving head-on face was about 1 m. The three-dimensional coordinates of source were 3864514 m, 39479034 m and -860 m, respectively. The horizontal distances between source and 1#, 3#, 4# and 8# sensors were 242 m, 1298 m, 982 m, and 1485 m. Fig.2 is the location relation sketch between source and 1#, 3#, 4#, and 8# sensors. The horizontal distance of source to 3# sensors is about 3.5 times that of source to 1# sensor, and is approximately equal to the distance between source and 4# sensor. Fig. 3 shows the amplitude spectrum-frequency curves of three-component signals recorded by 1#, 3#, 4#, and 8# sensors, where the horizontal logarithmic coordinate (logarithmic scale=7) was used.

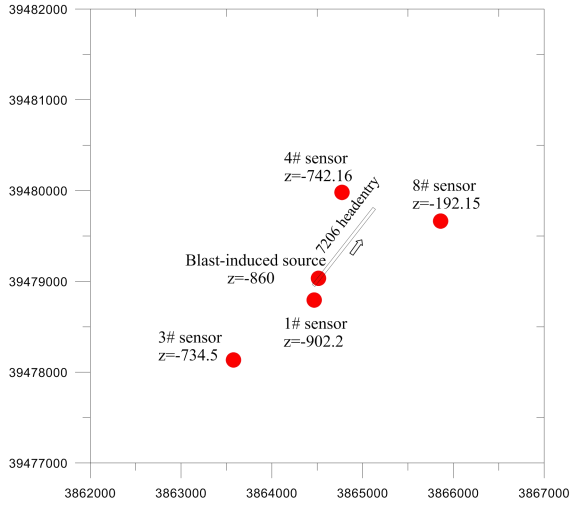

Fig.2. The location relation sketch between blast-induced source and sensors.

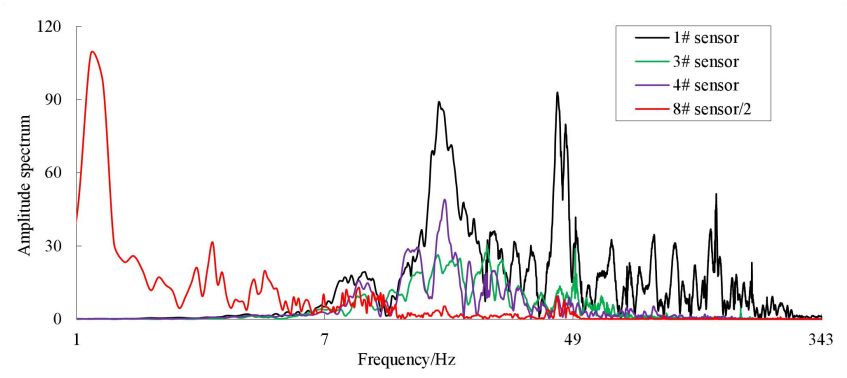

(a) Horizontal *x*-direction

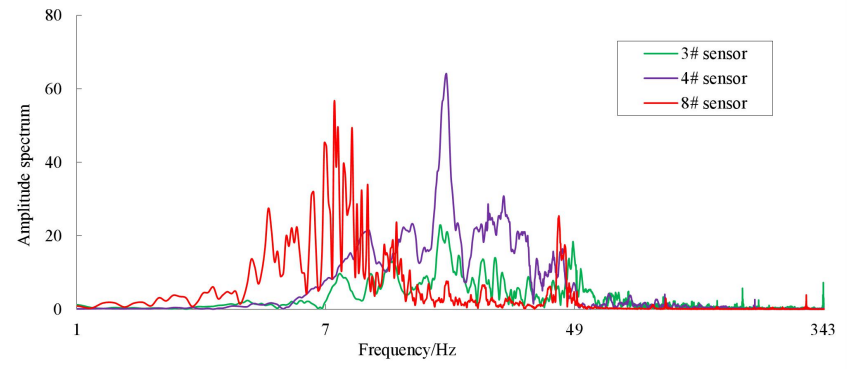

(b) Horizontal *y*-direction

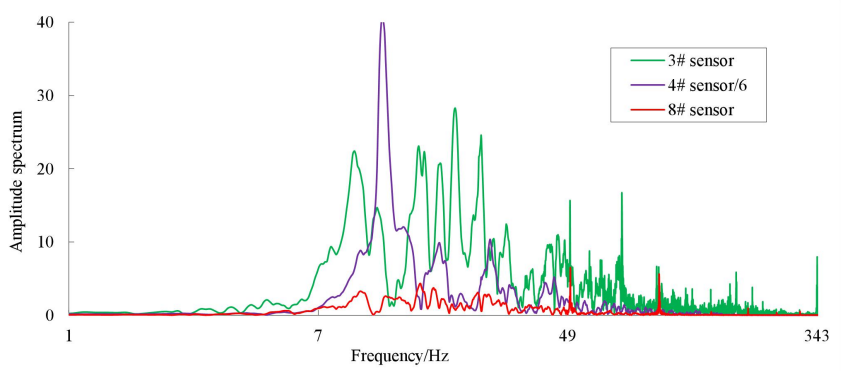

(c) Vertical *z*-direction

Fig.3. Amplitude spectrum- frequency curves of three-component signals of shock waves (Oct 25).

From Fig.3, along with blast-induced vibration wave propagation in coal and rock materials, due to the attenuation effect of fissures in the original coal and rock, goaf, and roadways, the high-frequency components of shock wave rapidly attenuated, and the frequency spectrum moved to low-frequency band. Simultaneously, the intensity of signal obviously reduced along with the increasing propagation distance, especially, for 8# sensor installed in based-surface deep borehole, the predominant frequency of signals after attenuation was less than 10 Hz, which indicated that the energy mainly concentrated in lower frequency band. Based on the signal intensity recorded by 1#, 3#, and 4# sensors, from the view of *x* and *y* horizontal directions, it can be known that when the increase of horizontal propagation distance was 3 times, the maximum-amplitude energy attenuation was nearly 1 time. Similarity, when the increase of horizontal propagation distance was 4.4 times, the maximum-amplitude energy attenuation was nearly 2 times. Especially, the propagation distance of shock wave increased 300 m, and the horizontal-directional energy attenuation was nearly 1.8 times. According to the vertical-directional energy of 1#, 3#, 4#, and 8# sensors, when the increase of vertical propagation distance was 0.06 times, the maximum-amplitude energy attenuation was nearly 7.6 times. Similarity, when the increase of vertical propagation distance was 4.6 times, the maximum-amplitude energy attenuation was nearly 30 times.

In summary, according to the attenuation level of shock wave propagation, the vertical attenuation coefficient of transverse propagation is much larger than bed-parallel horizontal attenuation coefficient. Especially, for the same propagation distances, there is a significant difference of 15 times between horizontal and vertical energy attenuation coefficients.

To further reveal and understand the attenuation coefficient variation law of shock wave in the horizontal and vertical directions, the relationship between amplitude spectrum and the propagation distance of shock wave was clearly demonstrated by regression analysis (in Fig.4).

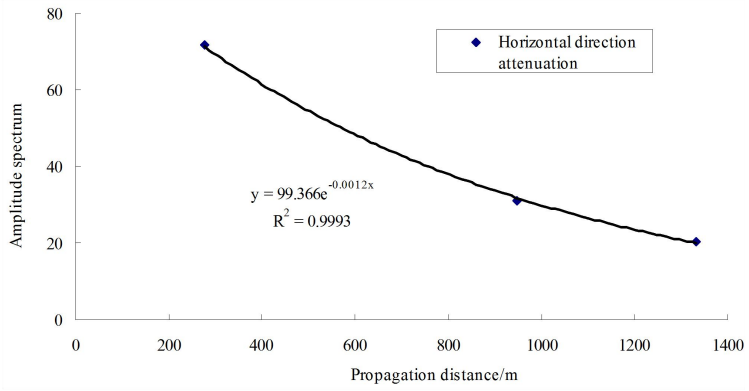

(a) Horizontal directional attenuation rule

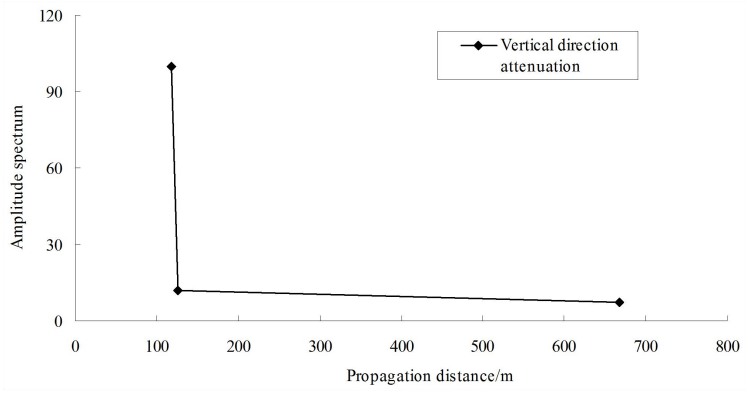

(b) Vertical directional attenuation rule

Fig.4. Horizontal and vertical directional attenuation rules generated by goaf and roadways.

From Fig.4, when shock wave propagated in the horizontal direction, the amplitude spectrum of residual wave showed the tendency of continuous and stable decreasing, and a negative exponential function whose bottom number is e was presented by regression analysis (the attenuation level coefficient is -0.0012). However, for the vertical direction propagation, the amplitude spectrum showed the mutation phenomenon to a great extent due to the severe attenuation effect of goaf and roadway between source and sensors. Without goaf and roadway in the vertical direction of propagation, the attenuation effect will dramatically mitigate.

3. Conclusions

By the methodology of field measurements, the attenuation and frequency-spectrum evolutionary rules of shock waves generated by blast were analyzed in 7206 working face of SCM. We obtained main conclusions are as:

(1) The vertical attenuation coefficient of transverse propagation is much larger than bed-parallel horizontal attenuation coefficient. Especially, for the same propagation distances, there is a significant difference of 15 times between horizontal and vertical energy attenuation coefficients.

(2) With shock wave propagation, the high-frequency components gradually attenuate, and the frequency spectrums move to the low-frequency band.

(3) A negative exponential function between the horizontal propagation distance and the intensity of residual shock wave is presented by regression analysis. However, for the vertical directional propagation, the amplitude spectrum manifests the mutation phenomenon to a great extent due to the severe attenuation effect of discontinuity structures such as goaf and roadways vertically between source and sensors.

Acknowledgments

The authors wish to express they’re thanks to the collaborative funding support from the Project Funded by the Priority Academic Program Development of Jiangsu Higher Education Institutions (SZBF2011-6-B35).

References

[1] Bollinger GA (1971) Blast vibration analysis. Southern Illinois University Press.

[2] Chen G, Huang S (2001) Analysis of ground vibrations caused by open pit production blasts: a case study. Fragblast-International Journal of Blasting and Fragmentation 5: 91–107.

[3] Siskind DE, Stagg MS, Kopp JW, et al (1980) Structure response and damage produced by ground vibrations from surface mine blasting. USBM RI 8507.

[4] Anderson DA, Winzer SR, Ritter AP (1982) Blast design for optimizing fragmentation while controlling frequency of ground vibration. In: Proceedings of the 8th Conference on Explosives and Blasting Technique. New Orleans, p 69–89.

[5] Dowding CH (1985) Blast vibration monitoring and control. Prentice-Hall, Inc., Englewood Cliffs, NJ.
[6] Khandelwal M, Singh TN (2006) Prediction of blast induced ground vibrations and frequency in opencast mine: A neural network approach. Journal of Sound and Vibration 289: 711–725.
[7] Wei XY, Zhao ZY, Gu J (2009) Numerical simulations of rock mass damage induced by underground explosion. International Journal of Rock Mechanics & Mining Sciences 46: 1206–1213.
[8] Khandelwal M (2010) Evaluation and prediction of blast-induced ground vibration using support vector machine. International Journal of Rock Mechanics & Mining Sciences 47: 509–516.